Radio Frequency Gas Breakdown and Micro/Nano-Plasma Formation in High-Power Evanescent-Mode Cavity Resonators

Abbas Semnani and Dimitrios Peroulis

School of Electrical and Computer Engineering, Birck Nanotechnology Center
1205 West State Street, West Lafayette, IN 47907, USA
asemnani@purdue.edu, dperouli@purdue.edu

Abstract

Microwave gas breakdown may limit power handling in antennas and RF resonators that store electromagnetic energy in micro/nano-gaps. In this paper, we review the numerical modeling and experimental validation of RF gas breakdown in evanescent-mode cavity resonators. This type of resonator stores the majority of its electric field energy in a micron-sized gap. High RF power-induced gas breakdown may degrade its performance by shifting the resonant frequency and/or increasing its insertion loss by eroding the micron-size-gap forming electrodes. Both static and tunable resonators are studied by RF plasma simulation techniques and the results are experimentally validated by high power measurements.

1. Introduction

Electronically-tunable evanescent-mode (EVA) cavity resonators have recently attracted a lot of interest due to their wide range of tunability, narrow instantaneous bandwidth, low insertion loss, high quality factor (Q), and relatively small size. These essential characteristics have resulted in a number of unique and high-performance adaptive filters over the last five years [1-7].

Several applications such as satellite communication systems, base-station transmitters and radars require high power transmitting to increase the coverage and system performance. Two different issues may influence the high-power behavior of EVA resonators: a) non-linear electromechanical effects and b) RF gas discharge. Non-linear electromechanical effects are important in a tunable EVA resonator only when it includes a flexible diaphragm whose deflection controls its critical RF gap and consequently its resonant frequency. Specifically, when the RF field in the critical RF gap becomes comparable to the bias force applied to the diaphragm, non-linear effects may dominate its performance [5]. On the other hand, gas discharge and eventually breakdown due to strong RF electric field (E-field) affect both static and tunable EVA resonators [8]. Gas breakdown causes plasma formation which is electrically conductive and leads to both resonant frequency shift and insertion loss increase of the resonator.

In this paper, we review gas breakdown in EVA cavity resonators with micron/nano-sized critical gaps. Plasma simulations are performed to investigate the breakdown power and the post-breakdown conditions. Simulation results are also validated with high-power experimental ones.

2. Evanescent-Mode Cavity Resonator

As shown in Fig. 1, an EVA cavity resonator is often formed by placing a post at the center of a simple cavity resonator. Loading a simple cavity with such a post results in two main features. First, the size of EVA cavity resonator is significantly reduced for a given resonant frequency compared with a simple cavity resonator. Although this happens at a penalty of a lower quality factor, the resulting Q is typically in the order of 500-1,000 [1, 2, 5] which is sufficient for several applications. Second most of the E-field energy in an EVA is concentrated in the small volume between the post

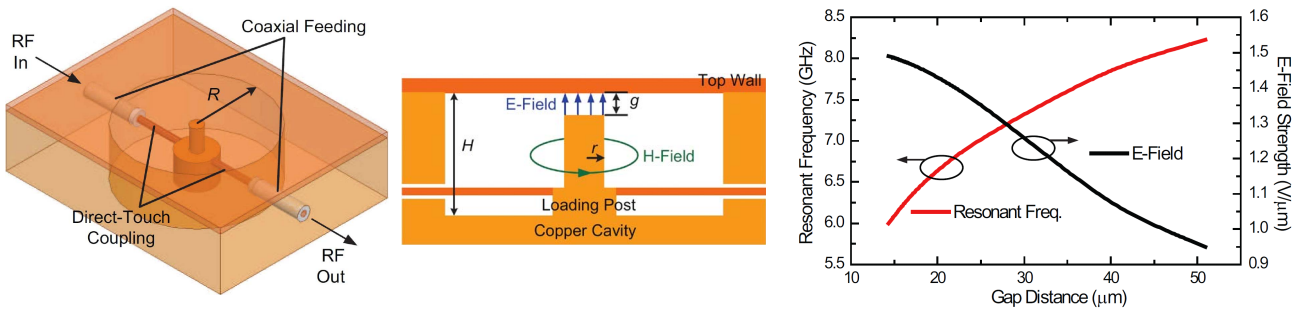

Fig. 1. Schematic of a typical EVA cavity resonator (left) and related parameters (middle). Simulated resonant frequency and normalized gap E-field versus different gap sizes (Case #2 in Table I) (right) [9].

978-1-4673-5225-3/14/$31.00 ©2014 IEEE

Table I
Finalized Parameters of the Cavities

Parameter	Case #1	Case #2
Post Diameter, r	0.42 mm	0.9 mm
Gap, g	19 µm	14.8-51.2 µm
Cavity Depth, H	4.5 mm	4.5 mm
Cavity Diameter, R	6 mm	12 mm

and the upper cavity wall. The resulting quasi-static capacitor can be tuned by changing this gap size to yield a frequency-agile resonator [1, 2, 7].

Fig. 1 also shows the simulated resonant frequency as well as the E-field magnitude over the gap (g) for an EVA resonator (Case #2 in Table I) with 1 W input power. It is observed that in this resonator, the resonant frequency is tuned from 6 to 8.2 GHz when the gap size is increased from 14 to 51 µm. Also, the E-field strength is decreased for larger gap sizes.

3. Micro/Nano-Plasma Simulation

Gas discharge is due to the generation of charged particles (electrons and ions) as a result of three main mechanisms of a) electron-impact ionization, b) secondary electron emission, and c) field emission [10, 11]. These particles are also lost as a result of recombination, attachment, as well as diffusion and drift to the electrodes. An avalanche increase in the number of particles occurs when the generation rate exceeds the loss leading to gas breakdown. Plasma formation in the center of the gap is the result of gas breakdown. While both DC and RF fields can ignite gas discharge, the relative contribution of each discharge mechanism depends mainly on the gap size (g), gas pressure and frequency [11, 12].

In this work, we use the one-dimensional particle-in-cell/Monte Carlo collision (PIC/MCC) technique [13] for the simulation of gas discharge. In this technique, a group of particles is represented by a single superparticle. In the PIC method, all superparticles are tracked in each time step by considering the applied forces, previous positions and velocities. The probable collisions are addressed with the MCC technique in which, the cross sections of different particles are considered for probable collisions. The simulation results in this work are based on the assumptions that Nitrogen gas at room temperature and atmospheric pressure exists between copper electrodes. Fig. 2 shows the simulated electrons and ions number densities, as well as E-field and potential over a 19 µm gap after microwave breakdown at 6.5 GHz [8].

4. Microwave Gas Breakdown

In order to evaluate the high frequency micro-gas breakdown and plasma formation in EVA cavity resonators, we consider two cases: a) a static one at 6.5 GHz, and b) a tunable resonator at 6-8.5 GHz. Considering the first case (Case #1 in Table I.), the gap size is 19 µm and PIC/MCC simulations show the peak breakdown field (E_{bd}) of 7.9 V/µm. Fig. 3 shows the high-power breakdown results for this case [8]. It is observed that when input power is increased, the insertion loss is almost constant up to the breakdown power at 45.3 dBm where it is increased by about 11 dB. This is due to the formation of a highly-conductive micro-plasma region inside the gap-restricted volume. This effect is also seen in the frequency response of the resonator when the input power goes beyond the breakdown power. Long-term erosion effects of gas breakdown when associated with ion bombardment are observed in Fig. 3, which is related to another static resonator with 32 µm gap working at 7.5 GHz.

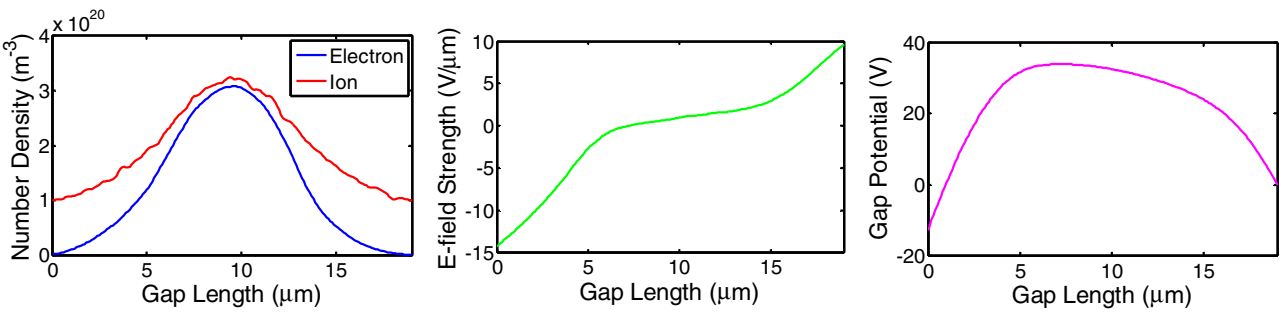

Fig. 2. Simulated average particles number density, magnitude of E-field and potential distribution over the gap of Case #2 after gas breakdown [8].

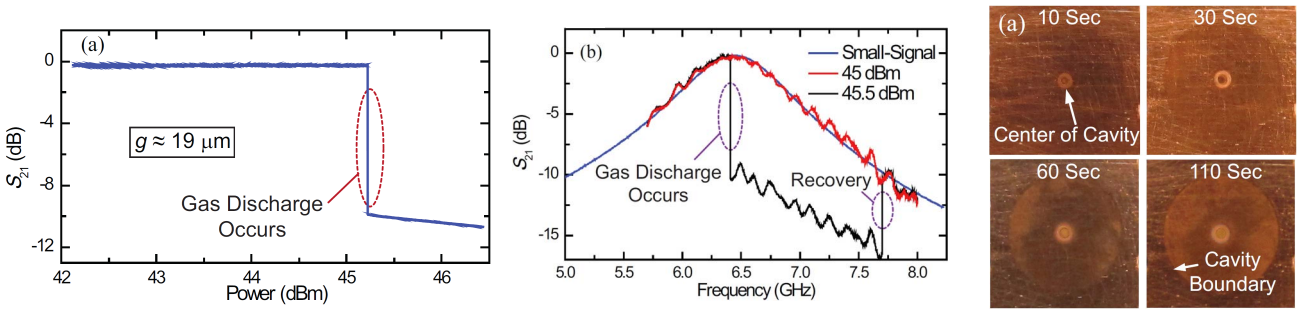

Fig. 3. Measured breakdown point in both power and frequency sweep modes for Case #1 (left and middle). Long term breakdown erosion effects for a 7.5 GHz resonator with 32 μm gap (right) [8].

Fig. 4 represents the measurement of breakdown power for different gap size/frequency of several static resonators (Case #2 in Table I) [9]. As expected, the breakdown power increases with the gap size. In addition, Fig. 4 shows that the high-frequency breakdown voltage simulated by the PIC/MCC method is in good agreement with the measurement results and is almost linearly increasing with the gap size.

5. Conclusion

This paper summarizes simulation and experimental results of gas micro-breakdown in evanescent-mode cavity resonators. This important phenomenon controls power handling in a wide variety of resonant RF devices that are based on storing electromagnetic energy in micro/nano-gaps. In the studied EVA resonators, this occurs when the RF E-field in the critical gap reaches a few V/μm. The high-frequency plasma simulations are performed by using the PIC/MCC technique. The predicted breakdown powers are in good agreement with the high power measurements for both static and tunable resonators. The breakdown voltage increases almost linearly with the gap size (frequency). Long-term erosion effects are clearly observed around the plasma region when ion bombardment is associated with the plasma formation.

6. Acknowledgments

This paper is based on work supported by the National Science Foundation under Grant No. ECS-1202095.

7. References

1. H. Joshi, H. H. Sigmarsson, S. Moon, D. Peroulis, and W. J. Chappell, "High-Q fully reconfigurable tunable bandpass filter," *IEEE Trans. Microw. Theory Tech.*, vol. 57, no. 12, pp. 3525-3533, Dec. 2009.

2. E. J. Naglich, J. Lee, D. Peroulis, and W. J. Chappell, "Switchless tunable bandstop-to-all-pass reconfigurable filter," *IEEE Trans. Microw. Theory Tech,* vol. 60, no.5, pp. 1258-1265, May 2012.

3. S. Fouladi, F. Huang, W. D. Yan, and R. R. Mansour, "High-Narrowband Tunable Combline Bandpass Filters Using MEMS Capacitor Banks and Piezomotors," *IEEE Trans. Microw. Theory Tech,* vol. 61, no.1, pp. 393-402, Jan. 2013.

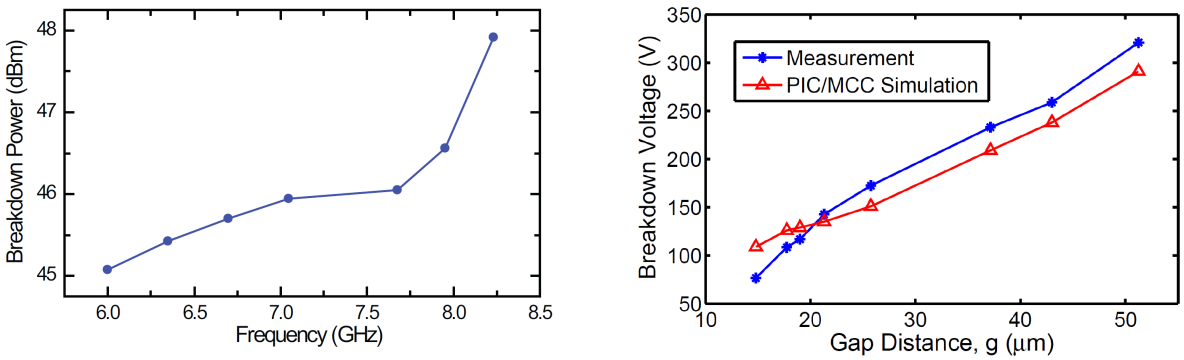

Fig. 4. Measured input breakdown power (left), as well as measured and simulated breakdown voltages (right) for Case #2 [9].

4. E. J. Naglich, J. Lee, D. Peroulis, and W. J. Chappell, "A tunable bandpass-to-bandstop reconfigurable filter with independent bandwidths and tunable response shape," *IEEE Trans. Microw. Theory Tech.*, vol. 58, no. 12, pp. 3770-3779, Dec. 2010.

5. X. Liu, L. P. Katehi, W. J. Chappell, and D. Peroulis, "Power handling of electrostatic MEMS evanescent-mode (EVA) tunable bandpass filters," *IEEE Trans. Microw. Theory Tech.,* vol. 60, no. 2, pp. 270-283, Feb. 2012.

6. S. J. Park, I. Reines, C. Patel, and G. M. Rebeiz, "High-RF-MEMS 4–6-GHz tunable evanescent-mode cavity filter," *IEEE Trans. Microw. Theory Tech.,* vol. 58, no. 2, pp. 381-389, Feb. 2010.

7. J. Lee, E. J. Naglich, H. H. Sigmarsson, D. Peroulis, and W. J. Chappell, "Tunable inter-resonator coupling structure with positive and negative values and its application to the field-programmable filter array (FPFA)," *IEEE Trans. Microw. Theory Tech.*, vol. 52, no. 12, pp. 3389-3400, Dec. 2011.

8. K. Chen, A. Semnani, and D. Peroulis, "High-power microwave gas discharge in high-Q evanescent-mode cavity resonators and its instantaneous and long-term effects," *Proc. IEEE MTT-S International Microwave Symposium*, June 2013.

9. A. Semnani, K. Chen, and D. Peroulis, "Microwave gas breakdown in tunable evanescent-mode cavity resonators," *Proc. IEEE Microwave and Wireless Component Letters*, (accepted).

10. M. A. Lieberman and A. J. Lichtenberg, *Principle of Plasma Discharge and Materials Processing*, New York: J. Wiley & Son, 2005.

11. A. Semnani, A. Venkattraman, A. A. Alexeenko, and D. Peroulis, "Pre-breakdown evaluation of gas discharge mechanisms in microgaps," *Applied Physics Letters*, vol. 102, no. 17, pp. 174102, 2013.

12. A. Semnani, A. Venkattraman, A. A. Alexeenko, and D. Peroulis, "Frequency response of atmospheric pressure gas breakdown in micro/nanogaps," *Applied Physics Letters*, vol. 103, no. 6, pp. 63102, 2013.

13. C. K. Birdsall, "Particle-in-cell charged-particle simulations, plus Monte Carlo collisions with neutral atoms, PIC-MCC," *IEEE Transactions on Plasma Science*, vol. 19, no. 2, pp. 65–85, 1991.